Int. J. Radiat. Biol., Vol. 86, No. 7, July 2010, pp. 593–601

informa
healthcare

Development of a method for assessing non-targeted radiation damage in an artificial 3D human skin model

GIUSEPPE SCHETTINO[1], GARY W. JOHNSON[2], STEVE A. MARINO[2], & DAVID J. BRENNER[2]

[1]*Centre Cancer Research and Cell Biology, Queen's University Belfast, Belfast, Northern Ireland, UK, and* [2]*Center for Radiological Research, Columbia University, New York, NY, USA*

(Received 16 July 2009; Revised 12 February 2010; Accepted 17 February 2010)

Abstract

Purpose: Despite the increasing concern about the effect of doses below 0.5 Gy and non-targeted exposures of ionising radiation on living organisms, the majority of radiobiological studies are conducted using in vitro cell lines. In order to be able to extrapolate the in vitro results to in vivo models with confidence, it would be of great benefit to develop a reproducible tissue system suitable for critical radiobiological assays. This manuscript describes the development of a reliable protocol to harvest cells from tissue samples and investigate the radiation damage induced on a single cell basis.

Materials and methods: To validate this approach as a potential tool for bystander experiments, the method focuses on analysing radiation damage in individual cells as a function of their relative position in the tissue. The experiments reported describe the micronucleus formation following partial irradiation with 3.5 MeV protons (0.1, 0.5 and 1 Gy) in an artificial human skin construct.

Results: The reproducible and low background frequency of micronuclei measured in this system allows detection of small increases following radiation exposures. The effect was statistically significant at doses as low as 0.1 Gy in the directly irradiated as well as in the bystander cells.

Conclusions: The data presented provide evidence of a spatially dependent bystander effect whose magnitude decrease as a function of the distance from the directly exposed area.

Keywords: *bystander effect, 3D skin tissue, micronuclei, protons*

Introduction

In recent years, increasing evidence has been reported regarding non-targeted radiation effects, attracting considerable interest in the radiotherapy and radioprotection community and assuming a primary role in modern radiobiology studies. Non-targeted radiation effects are classified as effects caused by ionising radiation in cells or samples which have not been directly exposed or in other words, which do not exhibit DNA (deoxyribonucleic acid) damage caused as a direct consequence of the ionisation tracks. Among them, the radiation-induced bystander effect is very well documented and has been widely investigated for different biological end-points in a variety of in vitro cell lines (Morgan and Sowa 2007). The bystander phenomenon refers to effects detected in cells that have not been directly exposed to ionising radiation but that have either shared medium with or been in contact with directly irradiated samples. Despite the fact that the underlying mechanisms are still not well understood, strong evidence has been accumulated suggesting a critical role played by gap-junction inter-cell communication (Azzam et al. 2001) as well as soluble factors released by the directly exposed samples such as cytokines (Iyer and Lehnert 2000) reactive oxygen species (ROS) (Tartier et al. 2007) and nitric oxide (NO) (Shao et al. 2003, Chen et al. 2008). The effects reported are generally dose-independent and despite being significantly smaller than those induced by direct radiation exposure, they may be of

Correspondence: Dr. Giuseppe Schettino, CCRCB, Queen's University Belfast, 97 Lisburn Road, Belfast, Northern Ireland, UK BT9 7BL. Tel: +44 2890 972940. E-mail: g.schettino@qub.ac.uk

ISSN 0955-3002 print/ISSN 1362-3095 online
DOI: 10.3109/09553001003734535

critical relevance in low-dose and/or non-uniform irradiation conditions. Such conditions are likely to arise in medical diagnostic/treatment or even common environment circumstances where the direct radiation damage component is expected to be very small. Moreover, the existence of the bystander effect poses a major challenge to DNA centred theories such as the target theory and the linear no-threshold hypothesis and seems to indicate the requirement for a paradigm shift in radiation biology. The new paradigms may have to take into consideration cell-to-cell and cell-to-matrix signalling to explain effects measured in cells not directly 'hit' by the radiation. Target sizes larger than the single cell itself and interactions over long distances and times will have to be considered a parameter as critical as the absorbed dose. It is therefore paramount to evaluate the relevance of the bystander effect for radiation protection and radiation therapy in a new multi-dimensional context.

In order to evaluate the significance of the bystander effect in terms of risk assessment to patients or regulation of the exposure level, in vitro results have to be validated in more complex biological systems that better represent in vivo models. The main issue in assessing the bystander response in in vivo models is the presence of other systematic factors that may mask the effect, making it impossible to attribute a specific phenotype found in unirradiated cells to the signal generated by directly exposed cells. Previous studies addressing this problem have used explant models (Belyakov et al. 2003) and in vitro tissue equivalents (Belyakov et al. 2005). Monolayer or two-dimensional explant models are of limited usefulness as they do not present the full three-dimensional tissue structure and/or differentiation pattern, offering only limited cell-cell interaction. On the other hand, tissue models that better resemble in vivo cell environments and interactions, present technical challenges for investigating long term radiation effects such as genomic instability. In order to accurately measure the contribution of the bystander effect to <0.5 Gy dose/partial irradiation of tissues, the samples have to be disaggregated into individual cells so that they may be further cultured, while still preserving their spatial correlation. Here, we report the bystander response in a 3-dimentional in vitro skin model partially exposed to 3.5 MeV protons. The same skin model has been previously used (Belyakov et al. 2005) to investigate in situ bystander response following microbeam irradiation. In this manuscript we present the development of a new experimental procedure for an in vivo-like assay to measure complex radiation damage on a single cell basis as a function of their relative position in the tissue. The study presented in this manuscript focuses on establishing the protocol working principal and comparing the micronuclei results with existing data to provide further insight into the relevance of the bystander effect in 3D biological samples.

Materials and methods

Tissue constructs

The experiments reported in this manuscript were performed using the EPI-200 tissue from MatTek Corporation (Ashland, MA, USA). The EPI-200 construct is a multilayered (8–12 cell layers, ~ 75 μm thick), differentiated tissue consisting of basal, spinous, granular and cornified layers with very similar microarchitectures to the corresponding tissue in vivo (Monteiro-Riviere et al. 1997). The EPI-200 tissue also exhibits mitotic and metabolic activity (Ponec et al. 2002), markers of specific differentiation (Zhao et al. 1999) and presence of gap junction (Netzlaff et al. 2005); characteristics of the in vivo epidermis. The tissue resembles the human epidermis as it is constructed from normal epidermal keratinocytes (foreskin-derived) with no fibroblasts and cultured on chemically modified, collagen-coated, 9 mm diameter culture inserts with porous membrane (MilliCell CM from Millipore Corporate, Billerica, MA, USA). The thickness of the insert membrane (~ 50 μm) was estimated by microscope measurements in the same conditions as for the irradiation setting (i.e., membranes blotted to remove excess medium and with sample growing on the top surface). Differentiation is induced by the air-medium gap by keeping the cell insert sitting just on top of the medium surface with the apical surface of the tissue exposed to the environment. The tissues were generally shipped overnight on Mondays and received on Tuesday mornings in 24-well trays. On arrival, the samples were placed in six-well culture plates, each containing 1 ml of fresh, pre-warmed New Maintenance Medium (NMM) from MatTek Corporation. The New Maintenance Medium was provided by MatTek Corporation and it is based on the Dulbecco's Modified Eagle's Medium (DMEM) with addition of keratinocytes growth factors (exact composition is proprietary of the manufacturer). The tissues were incubated at 5% CO_2 and 37°C for approximately 24 h before any experimental procedures took place. All samples come with a 'guaranteed long-term reproducibility' assured by internal tests performed by MatTek on samples from the same batch shipped to customers. Although occasional samples failing such tests were still used for irradiation tests, data from these experiments have not been included in this manuscript. A minimum of three samples were used for each experimental/irradiation conditions reported in this manuscript.

Irradiation

Tissue irradiation was performed using the Columbia University Radiological Research Accelerator Facility (RARAF) track-segment facility where a beam of 3.5 MeV protons emerges vertically through a thin scattering metal foil. The samples were irradiated from below (i.e., through the supporting membrane and from the dividing keratonocytes side). The tissue inserts were positioned in a custom-designed holder attached to a rotating wheel through which the samples can be scanned across the radiation beam (Bird et al. 1980). During the irradiation ($\sim$1 min/sample), the tissues were completely exposed to air. Dehydration was prevented by the supporting membrane being wet and by covering the tissue insert. No sign of dehydration was observed following the irradiation. In order to produce a spatially confined radiation exposure, a 100 μm thick platinum disk with a 50 μm wide slot across it, was placed directly below the tissue supporting membrane. The slot was aligned with the tissue insert to assure that only a narrow strip of the sample along its diameter was directly exposed to radiation. The portion of the tissue directly exposed to radiation was identified by marking the area of the supporting membrane corresponding to the slot on the platinum disk. Because of the little scattering of the 3.5 MeV protons as they pass through the platinum mask, the supporting membrane and the tissue ($\pm$15 μm as shown by Transport of Ions in Matter (TRIM) software simulation), the arrangement described above guarantees that cells more than a few tens of microns away from the irradiation area will receive no radiation dose. As the range of 3.5 MeV protons in tissue is around 190 μm, all layers of the portion of the tissue directly exposed will accumulate radiation dose. However due to the loss of energy of the protons as they pass through the sample, the top layer of cell will receive a dose higher ($\sim$20%) than that absorbed by the first layers, proportional to the change in the Linear Energy Transfer (LET) ($LET_{entrance} = 10.7$ keV/μm; $LET_{exit} = 12.9$ keV/μm). The dose reported in this manuscript refers to the dose absorbed by the cell in the first layers of the tissue sample.

Tissue slicing and cell harvesting

Following the irradiation, the tissue samples were immediately incubated in six multiwell plates in 2 ml of NMM containing either 1, 3, or 5 μg/ml Cytochalasin B (Sigma-Aldrich Corporation, St Louis, MO, USA) for 24, 48 or 72 h to block cytokinesis through the inhibition of actin function. The tissues could be kept in NMM for up to 5–7 days without significant alteration of their dividing and differentiating process as also confirmed by technical communication from MatTek Corporation. For the tissue slicing, the samples were removed from the culture insert by cutting off the entire supporting membrane using a scalpel. The tissue-membranes were then sliced using a custom designed microtome. The microtome (shown in Figure 1) was designed and manufactured by the Center for Radiological Research (Columbia University, New York, NY, USA) workshop specifically for such application (i.e., slicing of live tissue samples).

It basically consists of a vertically sliding razor blade that can be manually pressed against the tissue placed on a micrometer controlled platform. The tissues are placed face-up on the platform (which can accurately rotate to align the irradiated part of the sample with the blade under microscopic view, $\times$10 objective) with the surface tension between the plastic platform and the tissue supporting membrane enough to prevent sample movement during the slicing process. As the irradiated area is clearly marked (supporting membrane marked using the 50 μm wide slot of the irradiation set-up), its position is defined with a few 100s micron precision. The slice width is controlled by adjusting the platform position under the blade using a micrometer orthogonally orientated with respect to the blade itself (5 μm resolution). The EpiDerm tissue could be easily sliced down to 50 μm wide strips although the tissues have been cut to a minimum of 200 μm wide slices in the experiments reported in this manuscript to obtain a suitable number of cells/slice for the micronuclei study. By exerting the right pressure on the blade, it is possible to cut only the tissue while keeping the supporting membrane (which is harder to cut) intact. The tissue slices can then be easily peeled off the membrane by using a pair of forceps and performing under magnification

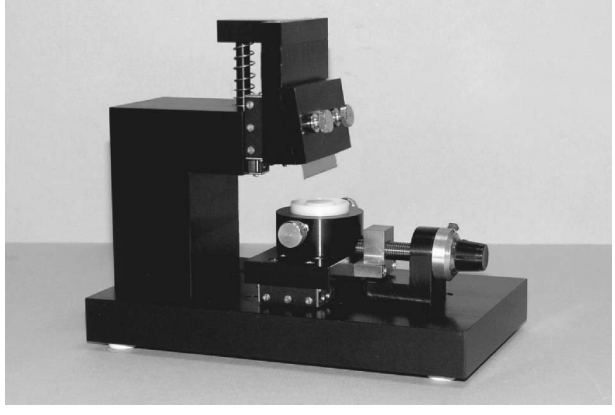

Figure 1. Customer designed microtome used for the tissue slicing. Microtome overall dimensions (width $\times$ length $\times$ height) = 10 $\times$ 20 $\times$ 18 cm

(×10). During this process, the samples are kept moisturised by a small drop (~50 μl) of NMM. For the work described in this manuscript, the Cytochalasin B treatment precedes the tissue slicing; however, the two operations can easily be inverted in case it is desirable to keep different part of the tissue isolated immediately after the radiation exposure.

Cells from each individual tissue slice were isolated and further processed for the micronuclei assay using the following protocol:

- Each slice was gently washed in Phosphate Buffered Saline (PBS) (Sigma-Aldrich Corporation) solution and then submerged in a 1 ml epperdorf containing 200 μl of trypsin supplemented with ethylenediaminetetraacetic acid (EDTA) (0.1%) (Sigma-Aldrich Corporation) and incubated for 30 min with frequent shaking;
- 0.5 ml of DMEM (Sigma-Aldrich Corporation) with 10% serum was added to neutralise the trypsin action;
- The cells were then gently centrifuged for 10 min at 450 *g* force;
- After the centrifugation, the supernatant was carefully removed and the cell pellet loosened with gentle agitation in 1 ml of fixative (3:1 methanol: acetic acid (Sigma-Aldrich Corporation), cold and freshly prepared);
- Cells were incubated at 4°C for 20 min;
- The cell suspension was then centrifuged again (10 min at 450 *g* force) and the supernatant discarded;
- The pellet was finally re-suspended in a fresh drop of fixative (~20 μl) and then gently pipetted onto a dry microscope slide. One slide was prepared for each tissue slice;
- The glass slide was left to dry at room temperature for several minutes;
- Slides were then rinsed in PBS and allowed to dry before being stained with Acridine Orange (Sigma-Aldrich Corporation).

Micronuclei scoring

For the micronuclei scoring, cells were stained using Acridine Orange at a final concentration of 0.25 mg/ml in PBS solution for 10 min at room temperature in the dark. The slides were subsequently washed with PBS, dried and assembled with a cover slip using VECTASHIELD Mounting Medium with 4′,6-diamidino-2-phenylindole (DAPI) (1.5 μg/ml) (Vector Laboratories, Burlingame, CA, USA). A minimum of 900 cells per sample were scored in order to determine the fraction of binucleated cells and the percentage of binucleated cells with micronuclei. The Fenech's criteria (Fenech 2000) was used to identify micronuclei.

Results

Tissue dissociation

The enzymatic dissociation treatment previously described was optimised with the aid of a personal communication with the MatTek Corporation and using existing dissociation protocols reported in literature (Curren et al. 2006). The procedure is relatively quick (less than 1.5 h per sample) while supplying a very high number of individual cells suitable for a variety of radiation damage assays. Overall, the average number of individual cells obtained was $\sim 2.5 \times 10^5$ cells/sample with more than 90% viable as by trypan blue exclusion test. The number of cells extracted was in excellent agreement with the number of cells composing the tissue as suggested by MatTek Corporation. Microscopic analysis of the small 'pad' of tissue remaining at the end of the enzymatic dissociation also supported such a conclusion. The 'pad' generally consisted of only the stratum corneum layer of skin with keratinocytes occasionally observed. This suggested that we were able to collect almost all cells of interest from the tissue sample with a high level of integrity as required for the determination of radiation damage. Although the trypsin incubation adopted for these experiments is longer (30 min) than what conventionally used in culturing established cell lines (few minutes), similar protocols have been successfully used. Exposure to trypsin solution up to 1 h are commonly used and suggested for the dissociation of human biopsies (Hybbinette et al. 1999) resulting in high number of cells with good proliferative potentials. A 35-min trypsin treatment, in particular, has been demonstrated to be suitable for similar MatTek systems for a variety of biological end-points including micronuclei formation (Curren et al. 2006). The high fractions of dissociated cells which successfully continue to proliferate support the hypothesis that although extensive, the trypsin treatment does not significantly alter the cell metabolism.

Cytochalasin-B treatment

Preliminary experiments were conducted to optimise the Cytochalasin B concentration required to provide a reasonable number of binucleated cells for the micronuclei assessment. This was determined by incubating the EpiDerm tissue in NMM containing Cytochalasin B at different concentrations for different incubation periods. The data was also used to establish the optimum Cytochalasin B conditions to use for the irradiation experiments. In this study, formation of binucleated cells up to a period of 72 h (i.e., about three average keratinocytes cell cycles) following exposure to three different concentrations of Cytochalasin B (i.e., 2, 3 and 5 μg/ml) were

analysed. As shown in Figure 2, incubation time and Cytochalasin B concentration both seem to increase the number of observed binucleated cells. At a concentration of 2 μg/ml, a rough linear increase of binucleated cells from $\sim$10% at 24 h to nearly 50% after 72 h was observed. For the 3 μg/ml concentration, the Cytochalasin B treatment induced about 30% of binucleated cells at 24 h which increased to reach a plateau at $\sim$60% at 48 and 72 h. Results not statistically different ($P > 0.05$ as for t-test) were obtained using a 5 μg/ml concentration (i.e., $\sim$40% binucleated cells at 24 h, 55% at 48 h and 61% after 72 h).

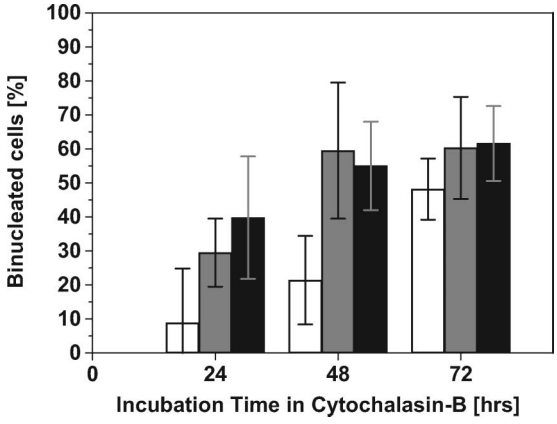

Figure 2. Induction of binucleated cells in EpiDerm tissue due to Cytochalasin B treatment. Concentration of 2 μg/ml (open bars), 3 μg/ml (gray bars) and 5 μg/ml (solid bars). Error bars indicate the standard error of the mean (SEM) for $n = 5$ independent experiments.

Although lower than what is generally achieved in monolayer cell-culture models (i.e., 70–80%), the data clearly showed that a reproducible and reasonable number of binucleated cells (1.3×10^5 binucleated cells per tissue sample) can be obtained with the protocol described. The number of cells is adequate for the analysis of micronuclei formation as well as a variety of other radiobiological end points. A final concentration of 3 μg/ml for 48 h was chosen for the irradiation experiments as longer times and higher concentrations do not produce a higher number of binucleated cells.

Bystander micronuclei induction

Determining the background response level is of critical relevance for the development of a new experimental protocol. In order to have a sensitive and robust model to accurately measure the small effects caused by bystander signals and dose exposures below 1 Gy, it is necessary to have a low and reproducible background response. The micronuclei level measured in the control samples is shown in Figure 3 where the fraction of binucleated cells with micronuclei is reported for each stripe into which the samples have been sliced into. The data indicate an average level of 0.72 ± 0.37% micronucleated cells. Such level is constant across the whole tissue and sufficiently low to conclude that no significant stress

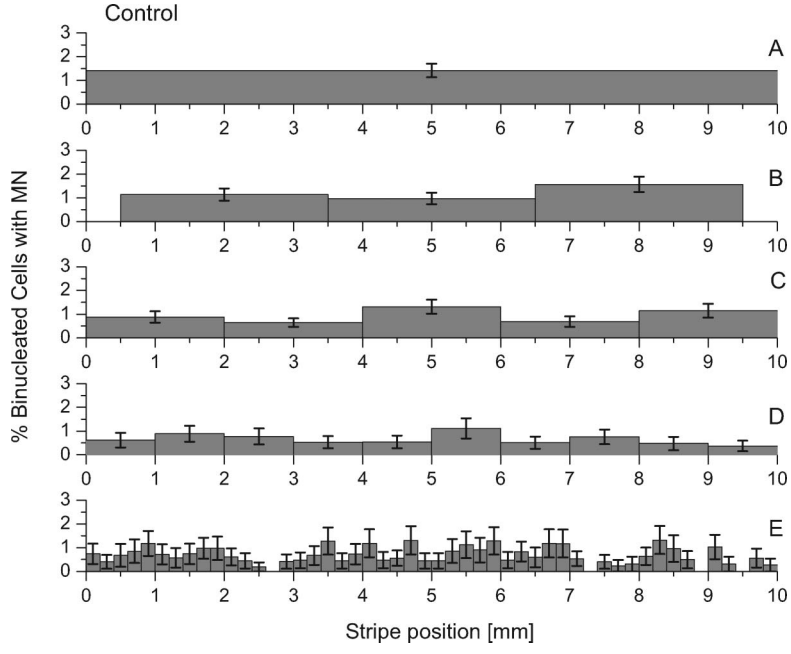

Figure 3. Frequency of micronuclei in unirradiated samples. Panel A, tissues were disaggregated into single cells without being sliced. Panel B, C, D and E, tissues were respectively sliced into 3 mm, 2 mm, 1 mm and 0.2 mm wide stripes before being individually disaggregated. The average frequency measured in our system is 0.72 ± 0.37% micronucleated cells. Error bars indicate the standard error of the mean (SEM) for a minimum of $n = 3$ independent experiments.

is induced by the above described protocol making it possible to measure small radiation responses. The effect of the stress induced by the slicing procedure has also been assessed by comparing the micronuclei level measured in the unsliced samples with those present in samples with multiple cuts. As shown, there is no statistical difference ($P > 0.05$) between the average micronuclei level measured in each of the controls reported.

Following a shielded irradiation (50 μm wide line across the tissue diameter) with 3.5 MeV protons, the bystander response has been evaluated by measuring the fraction of cells with micronuclei in each individual stripe which the tissues were sliced. The results are reported as a function of the stripe position relative to the irradiation line for three different dose points (0.1, 0.5 and 1 Gy). As reported for the controls, the effect of slicing the samples into different stripe sizes has also been investigated by grouping the data as a function of the number of stripes cut from each tissue (Figure 4). On average, more than 2000 cells per stripe were scored with the exception of the 0.5 mm stripes where only $\sim$1000 cells were analysed due to the lower number of cells recovered.

An increase in micronuclei formation was measured in almost all irradiated tissues with the maximum occurring in the stripes containing the directly irradiated cells (2.5–3.0% micronucleated cells). An elevated micronuclei level (expressed as percentage) was also evident in bystander stripes although the increase relative to the background was not always statistically significant according to equal variance *t*-test analysis (as reported in Figure 4). Interestingly, while larger differences from the controls have been measured in the tissue samples which have been sliced into fewer (i.e., larger) stripes, the deviation from the control data was in many case non-significant for the samples cut into narrower stripes. This effect was particularly evident for the 0.1 Gy – 0.5 mm stripe data (Figure 4 top graph panel C), where only the central directly irradiated stripe and a stripe in close proximity exhibit significant increased micronucleation ($P < 0.05$).

Finally, possible radiation induced cell cycle delay was assessed by monitoring the fraction of binucleated cells recovered. As shown in Table I, the radiation exposure does not appear to affect the fraction of binucleated cells either in the whole sample or in the individual stripe containing the directly irradiated cells.

Discussion

The objective of the work described in this manuscript was to develop a novel assay to measure direct and bystander radiation damage on an in vitro 3D human skin tissue model. The use of a biological model that closely resembles normal human tissue offers great potential for the investigation of non-targeted radiation effects in a more relevant environment, where cell signalling and direct cell-cell contact play a critical role. Although 3D models have already been used for similar studies, so far it has not been possible to investigate the bystander contribution for induction of critical DNA damage events. This was due to difficulty in performing single cell assays in tissues, while preserving their spatial correlation. We have used the described method to investigate the induction of micronuclei following partial irradiation (50 μm wide line across the tissue diameter) with 3.5 MeV protons in order to compare the results with available published data and demonstrate the feasibility of the protocol. The micronuclei assay has been chosen as there are extensive literature data (Prise et al. 1998, Belyakov et al. 2003) confirming the validity of an assay as the measure for bystander effect and offering suitable data for comparison in 2D systems (explants and isolated cell systems). The reproducibility of the data and the low level of damage detected in the control samples seem to support the use of such approach for the investigation of other biological endpoints.

The developed slicing and harvesting protocol has been shown to be able to recover a very large fraction of the tissue cells obtaining a still viable single cell solution. The number of cells recovered was in agreement with the number calculated with a simple geometrical approach and with the estimation provided by the tissue supply company (MatTek). The purpose-built microtome to slice live tissues has proved to be very precise and effective, easy to use and economically affordable. Three different Cytochalasin-B concentrations have been tested for an incubation time up to 72 h to determine the cell division rate and the best conditions for micronuclei scoring. The maximum number of binucleated cells was achieved for a 3 μg/ml concentration and 48 h incubation with no evident improvement for longer incubations or higher concentrations. Although the fraction of binucleated cells measured ($\sim$60%) was lower than that observed in the same in vitro cell cultures (this may be due to the longer trypsin treatment), it is still adequate to perform the proposed studies and the technique demonstrates that an overall viable single cell population was produced. Additionally, the background frequency of micronuclei scored in the control samples is considerably low (0.72 ± 0.37% of micronucleated cells) and very reproducible, making the model suitable for straightforward statistical analysis. The lack of increase in the micronuclei frequency in control samples which had been sliced compared to

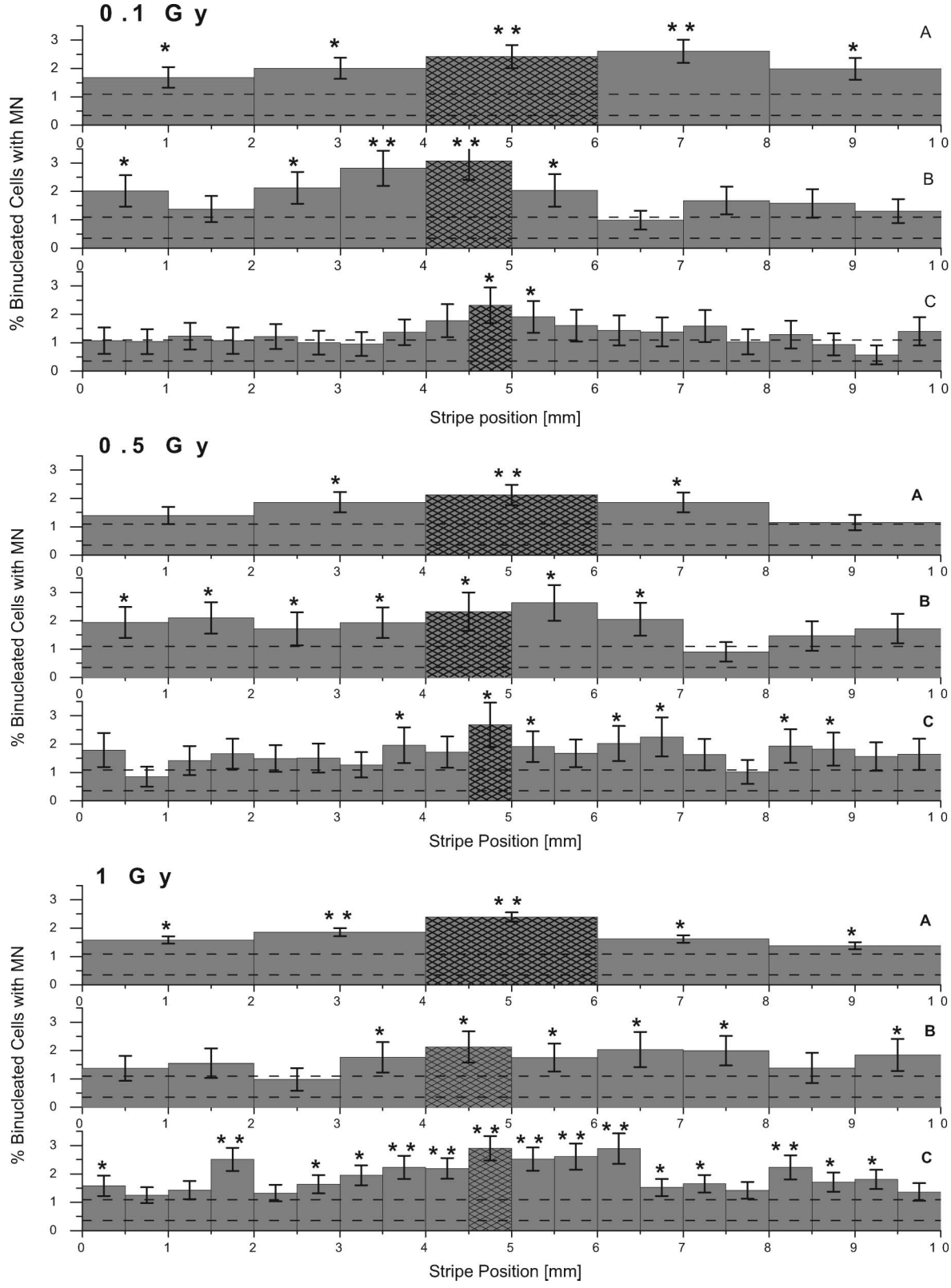

Figure 4. Frequency of micronuclei in irradiated samples (0.1, 0.5 and 1 Gy from top to bottom). Tissues sliced into 2 mm wide stripes are reported in panels A while data relative to 1 mm and 0.5 mm wide stripes are shown on panels B and C, respectively. As the directly irradiated area of the tissue is known within a few 100 s micron precision, the stripes containing the directly irradiated cells are highlighted. The average level of background micronuclei as measured in the control samples ($0.72 \pm 0.37\%$ micronucleated cells) is also shown (dashed lines). Error bars indicate the standard error of the mean (SEM) for minimum $n = 3$ independent experiments. Data statistical significant from average control value indicated with $\star (P < 0.05)$ and $\star\star (P < 0.01)$.

Table I. Fraction of average binucleated cells per sample measured with the above described protocol following partial irradiation exposures. Error bars indicate the standard error of the mean (SEM) for minimum $n = 3$ independent experiments.

	% Binucleated cells
Control (0 Gy)	66.2 ± 6.0
0.1 Gy	62.3 ± 5.6
0.5 Gy	66.0 ± 6.0
1 Gy	66.2 ± 7.4

that measured in intact tissues, also indicates that no considerable stress or alteration is introduced by the slicing process.

Partial irradiation of the samples resulted in an elevated micronuclei frequency not only in the stripes containing the direct irradiated cells but also in some of the adjacent stripes with unexposed cells. The damage detected in those cells cannot be attributed to the effect of proton scattering ($< \pm 15$ μm as from TRIM simulations) or secondary electrons (max energy ~ 7.5 keV, range < 2.5 μm). The magnitude of the bystander effect observed seems to be dose independent and clearly detectable in our 3D tissue models for doses as low as 0.1 Gy. Furthermore, the data indicate a higher level of micronuclei in the central portion of the sample (i.e., closer to the irradiation site) with evidence of a decreasing but still detectable effect towards the edges. This suggests a range for the bystander response of several millimetres, with potential critical consequences for radiotherapy and radioprotection as it essentially increases the volume and the number of cells affected. The results are in agreement with previous data (Belyakov et al. 2005) obtained irradiating the same biological system with a precise number of α-particles (microbeam irradiation) and scoring for micronuclei formation in fixed sliced sections of the tissue. The longer range of the damage reported in this manuscript (elevation of micronuclei detected up to a few millimetres from the irradiated area) could be accounted by the different irradiation exposures. While Belyakov and colleagues irradiated about 80 locations along the diameter of the sample (10 α-particles every 100 μm), our samples experienced a more uniform exposure (all cells along the 50 μm wide line across the sample diameter were irradiated). Considering also the higher penetration of 3.5 MeV protons (190 μm compared to 60 μm of 7.2 MeV α-particles), this implies a greater number of cells directly irradiated. The longer range of the damage measured could therefore suggest a link between the number of cells targeted and the strength of the bystander signal. On the other hand, the higher fraction of micronuclei detected in the central area of the sample and the long range of the effect, support the hypothesis that signal(s) are generated by the cells directly damaged by radiation and propagate cell-by-cell (whether they are damaged or not) with great efficiency. Due to the overall low level of damage induced ($< 3\%$ micronucleated cells), if the bystander signal were to be propagated only by the damaged cells (although with high efficiency), it would have been reasonable to expect a rapid decrease with distance from the irradiation site. The long range of the effect seems to suggest that cells that do not exhibit damage are also involved in the signal propagation.

Interestingly, almost no significant increase above the background level was measured for the 0.1 Gy – 0.5 mm stripes dose point. A possible explanation could lie in the different number of cells scored (~ 1000 samples for the narrow stripes against more than 2000 for all other cases) as forced by the lower number of cells recovered. However under the same experimental conditions (0.5 mm wide stripes), a significant bystander effect was detected for the 1 Gy dose point with the 0.5 Gy relative data showing an ambiguous response. Further investigations are required by expanding the dose range and/or by slicing the samples into finer stripes.

In conclusion, the excellent control levels, low variability and trend agreement with other bystander measurements in tissue systems indicate that the approach described in this manuscript is suitable for accurate bystander investigations in complex 3D samples. Compared to the traditional technique where the sample is left intact and then fixed/sectioned to score in situ damage, this method offers the flexibility to live section the samples at any time post irradiation (while preserving cell activities and proliferation for longer periods) to specifically address questions related to the transmission of extracellular signals. Moreover, dissociation of the samples and further culturing of single cells widen the range of biological end points while at the same time preserving same spatial information.

Acknowledgements

This work was supported by the P41 EB002033 grant (from the National Institute of Biomedical Imaging and Bioengineering [NIBIB]).

Declaration of interest: The authors report no conflicts of interest. The authors alone are responsible for the content and writing of the paper.

References

Azzam EI, de Toledo SM, Little JB. 2001. Direct evidence for the participation of gap junction-mediated intercellular communication in the transmission of damage signals from α-particle

irradiated to non-irradiated cells. Proceedings of the National Academy of Science of the USA 98:473–478.

Belyakov OV, Folkard M, Mothersill C, Prise KM, Michael BD. 2003. A proliferation-dependent bystander effect in primary porcine and human urothelial explants in response to targeted irradiation. British Journal of Cancer 88:767–774.

Belyakov OV, Mitchell SA, Parikh D, Randers-Pehrson G, Marino SA, Amundson SA, Geard CR, Brenner DJ. 2005. Biological effects in unirradiated human tissue induced by radiation damage up to 1 mm away. Proceedings of the National Academy of Science of the USA 102:14203–14208.

Bird RP, Rohrig N, Colvett RD, Geard CR, Marino SA. 1980. Inactivation of synchronized Chinese Hamster V79 cells with charged-particle track segments. Radiation Research 82: 277–289.

Chen S, Zhao Y, Han W, Zhao G, Zhu L, Wang J, Bao L, Jiang E, Xu A, Hei TK, Yu Z, Wu L. 2008. Mitochondria-dependent signalling pathways are involved in the early process of radiation-induced bystander effects. British Journal of Cancer 98:1839–1844.

Curren RD, Mun GC, Gibson DP, Aardema MJ. 2006. Development of a method for assessing micronucleus induction in a 3D human skin model (EpiDerm). Mutation Research 607:192–204.

Fenech M. 2000. The in vitro micronucleus technique. Mutation Research 455:81–95.

Hybbinette S, Bostrom M, Lindberg K. 1999. Enzymatic dissociation of keratinocytes from human skin biopsies for in vitro cell propagation. Experimental Dermatology 8:30–38.

Iyer R, Lehnert BE. 2000. Factors underlying the cell growth-related bystander responses to alpha-particles. Cancer Research 60:1290–1298.

Monteiro-Riviere NA, Inman AO, Snider TH, Blank JA, Hobson DW. 1997. Comparison of an in vitro skin model to normal human skin for dermatological research. Microscopical Research and Technology 37:172–179.

Morgan WF, Sowa MB. 2007. Non-targeted bystander effects induced by ionizing radiation. Mutation Research 616: 159–164.

Netzlaff F, Lehr CM, Wertz PW, Schaefer UF. 2005. The human epidermis models EpiSkin, SkinEthic and EpiDerm: An evaluation of morphology and their suitability for testing phototoxicity, irritancy, corrosivity, and substance transport. European Journal of Pharmaceutics and Biopharmaceutics 60:167–178.

Ponec M, Boelsma E, Gibbs S, Mommaas M. 2002. Characterization of reconstructed skin models. Skin Pharmacology and Applied Skin Physiology 15(Suppl. 1):4–17.

Prise KM, Belyakov OV, Folkard M, Michael BD. 1998. Studies of bystander effects in human fibroblasts using a charged particle microbeam. International Journal of Radiation Biology 74:793–798.

Shao C, Stewart V, Folkard M, Michael BD, Prise KM. 2003. Nitric oxide-mediated signalling on the bystander response of individually targeted glioma cells. Cancer Research 63: 8437–8442.

Tartier L, Gilchrist S, Folkard M, Prise KM. 2007. Cytoplasmic irradiation induces 53BP1 protein recolization in irradiated and bystander cells. Cancer Research 67:5872–5879.

Zhao JF, Zhang YJ, Kubilus J, Jin XH, Santella RM, Athar M, Wang ZY, Bickers DR. 1999. Reconstituted 3-dimensional human skin as a novel in vitro model for studies of carcinogenesis. Biochemical and Biophysical Research Communications 254:49–53.